

# i2LQR: Iterative LQR for Iterative Tasks in Dynamic Environments

Yifan Zeng<sup>\*1</sup>, Suiyi He<sup>\*2</sup>, Han Hoang Nguyen<sup>3</sup>, Zhongyu Li<sup>3</sup>, Koushil Sreenath<sup>3</sup>, Jun Zeng<sup>3</sup>

**Abstract**—This work introduces a novel control strategy called Iterative Linear Quadratic Regulator for Iterative Tasks (i2LQR), which aims to pursue optimal performance for iterative tasks in a dynamic environment. The proposed algorithm is reference-free and utilizes historical data from previous iterations to enhance the performance of the autonomous system. Unlike existing algorithms, the i2LQR computes the optimal solution in an iterative manner at each timestamp, rendering it well-suited for iterative tasks with changing constraints at different iterations. To evaluate the performance of the proposed algorithm, we conduct numerical simulations for an iterative task aimed at minimizing time consumption. The results show that i2LQR achieves the optimal performance as the state-of-the-art algorithm in static environments, and outperforms the state-of-the-art algorithm in dynamic environments with both static and dynamics obstacles.

## I. INTRODUCTION

### A. Motivation

One important objective of control algorithms is to optimize the performance of autonomous systems. This can be usually formulated as minimizing time [1] or energy consumption [2] during task execution. The performance-optimal controller can be applied to iterative tasks, where the autonomous system must do the same task repeatedly. However, the surrounding environment around the autonomous system may be dynamic. This means that constraints of the system are not always the same along the process, such as constraints that are changed in some given iterations, e.g., new obstacles appear after a particular iteration or moving obstacles in a single iteration. The existing state-of-the-art algorithm cannot handle these changes effectively. This motivates us to propose a control strategy that could handle additional constraints in different iterations while achieving the system’s optimal performance.

### B. Related Work

Researchers have applied different methods to address the problem of optimizing performance. Model-based approaches usually leverage a high-level planner to generate the optimal trajectory and a low-level controller is deployed to track the planned trajectory [3]–[6]. However, calculating the best possible or global optimal trajectory can be time consuming, and the low-level controller may not track the

trajectory perfectly due to discretization in the planning problem. Furthermore, when the planned trajectory encounters conflicts with newly appeared constraints, local re-planning is required to deal with these additional constraints [7]. This may result in the loss of global optimality for the trajectory.

Several attempts are made to address the problem through data-driven based model-free approaches, where the system’s historical data is used to train an end-to-end control policy directly. For instance, in [1], [8], the learning-based control policy shows its capability to push an autonomous racing car to its dynamics limit. In [9], [10], quadrotors are shown to fly with an aggressive maneuver in autonomous drone racing competition. Nevertheless, these methods still have limitations. Learning-based methods are data hungry and require significant time to get the policy, which means that such methods may not be suitable for some real-time applications. Moreover, all the aforementioned policies operate in a static environment. However, in practice, the control policy is required to be functional in a dynamic environment. More importantly, since the performance of the trained policy is highly related to the used training data set, the learned policy may not guarantee the global optimal performance.

Recently, reference-free model-based methods are proposed to provide optimal performance for iterative tasks. In [11], a model predictive contouring controller (MPCC) with dynamics learning is used for autonomous racing cars. The state-of-the-art algorithm, called learning-based MPC (LMPC), is introduced in [12], [13], where the system’s historical data is used to formulate the local MPC optimization problem. This allows the system to improve its performance along the iteration and the system is proved theoretically to achieve global optimal performance [12]. The proposed algorithm is implemented on autonomous vehicles [14], [15] and aerial robots [16]. However, these methods still have shortcomings. Although the local objective function in [11] considers optimal performance along the prediction horizon, the result is not global optimal without global planning. Moreover, the LMPC strategy in [12], [13] must work in a static environment, which means that the scenario should be exactly same for every iteration. This is due to the limitation of the optimization setup, where local MPC’s feasibility strictly depends on the reachability of historical states from previous iterations. If new obstacles are introduced, these historical states could be infeasible, rendering the MPC problem infeasible. One possible solution to this problem is local-replanning [17], but the performance may be limited due to the nonsmooth switch in the high-level planner.

To ensure that the autonomous system can smoothly adapt to newly introduced constraints, the optimal trajectory should

<sup>\*</sup>Authors have contributed equally.

<sup>1</sup>Author is with SJTU Paris Elite Institute of Technology, Shanghai Jiao Tong University, Shanghai, China. blakezyf1107@sjtu.edu.cn

<sup>2</sup>Author is with University of Minnesota-Twin Cities, MN 55455, USA. he000231@umn.edu

<sup>3</sup>Authors are with University of California, Berkeley. {hanhn, zhongyu\_li, koushil, zengjunsjtu}@berkeley.edu

TABLE I: Symbol Notations

Symbols for iterative tasks	
Symbol	Description
$\mathbf{x}_t^i$	System state at time step $t$ of iteration $i$
$\mathbf{u}_t^i$	System input at time step $t$ of iteration $i$
$\mathbf{x}_0$	Initial state of a single iteration
$\mathbf{x}_{\text{target}}$	Target state of a single iteration
$h(\mathbf{x}_t^i)$	Cost-to-go associated with system state $\mathbf{x}_t^i$
$\mathcal{X}^i$	Set of historical states for iteration $i$
$\mathcal{H}$	Set of all historical states from previous iterations
$\mathcal{C}_t^i$	Constraints on the system at time step $t$ in iteration $i$
$\epsilon$	A small positive number
Symbols for i2LQR	
Symbol	Description
$\tilde{\mathbf{x}}_r$	Guided state for $r$ -th target terminal set
$\mathbf{z}_r(j)$	$j$ -th state from $r$ -th target terminal set
$N$	Prediction horizon for the optimization problem
$\mathcal{Z}_r$	$r$ -th target terminal set
$\mathbf{x}_r^m(j)$	Open-loop states of $m$ -th iteration of iLQR for $\mathbf{z}_r(j)$
$\mathbf{u}_r^m(j)$	Open-loop inputs of $m$ -th iteration of iLQR for $\mathbf{z}_r(j)$
$\mathbf{x}_r^*(j)$	Optimized open-loop states from iLQR for $\mathbf{z}_r(j)$
$\mathbf{u}_r^*(j)$	Optimized open-loop inputs from iLQR for $\mathbf{z}_r(j)$
$\mathbf{x}_r^*(j_r^*)$	Best open-loop states for $r$ -th optimization cycle
$\mathbf{u}_r^*(x_r^*)$	Best open-loop inputs for $r$ -th optimization cycle
$J_t(\mathbf{x}_t^i, \mathbf{z}_r(j))$	Cost for nearest point selection on $\tilde{\mathbf{x}}_r$
$m_{\text{max}}$	Maximum iteration for iterative optimization
$r_{\text{max}}$	Maximum iteration for target terminal set

be computed in an iterative manner. Therefore, we want to use a method that could handle this without resulting in infeasibility. The iterative linear quadratic regulator (iLQR) shows potential in solving this problem. iLQR is an extension of LQR control, where the optimization is solved iteratively and linearization of cost function and system dynamics is conducted in each iteration. In [18], the iLQR computes the open-loop predicted trajectory for control problems with nonlinear dynamics and complicated constraints in an iterative manner. This motivates us to investigate the above challenging problem using an iLQR-based algorithm.

### C. Contribution

The contributions of this paper are as follows:

- We propose a novel optimal control strategy called Iterative LQR for Iterative Tasks (i2LQR), which provides optimal performance for a general dynamic system for iterative tasks in dynamic environments.
- We show how to use historical data from previous iterations to build the local optimization problem of i2LQR at each time step and how to solve this optimization problem in an iterative manner.
- Through numerical simulation, our proposed control strategy is shown to achieve the same optimal performance as state-of-the-art LMPC algorithm for iterative tasks in static environments and outperforms the LMPC algorithm for iterative tasks in dynamic environments.

## II. PROBLEM SETUP

In this section, we introduce the problem setup of iterative tasks. For an iterative task at time step  $t$  of iteration  $i$ , an autonomous system with dynamics  $\mathbf{x}_{t+1}^i = f(\mathbf{x}_t^i, \mathbf{u}_t^i)$  performs the task repeatedly until completion. In each iteration, the system starts from the same initial state  $\mathbf{x}_0$  and ends at the same target state  $\mathbf{x}_{\text{target}}$ . The system's historical data (e.g. state, time or energy consumption) is saved in a historical data set  $\mathcal{H}$ . The system's controller computes the optimal

input based on this data set  $\mathcal{H}$ , state  $\mathbf{x}_t^i$  and constraint  $\mathcal{C}_t^i$  at current time step. The constraint  $\mathcal{C}_t^i$  includes the constraints on both system states and inputs. If the system works in a static environment [13], [14], the constraint  $\mathcal{C}_t^i$  will be same for the same time step  $t$  of different iterations (i.e.,  $\mathcal{C}_t^i = \mathcal{C}_t^{i+1}$ ). If the system works in a dynamic environment (as in this work), the constraint  $\mathcal{C}_t^i$  will change along the entire process (i.e.,  $\mathcal{C}_t^i \neq \mathcal{C}_t^{i+1}$  or  $\mathcal{C}_{t+1}^i \neq \mathcal{C}_t^i$ ). A cost-to-go  $h(\mathbf{x}_t^i)$  is associated with each historical state. This describes the cost to finish the corresponding iteration from that point to the target state  $\mathbf{x}_{\text{target}}$ . The general form of this problem is shown in Alg. 1.

In this work, we focus on designing a performance optimal controller, which could minimize the cost  $h(\mathbf{x}_t^i)$  of the iterative task. Details about this algorithm will be illustrated in Sec. III. Parameters used in this work are listed in TABLE I along with their notations.

### Algorithm 1 Iterative Tasks

---

```

1:  $\mathcal{H} \leftarrow \emptyset$ 
2: repeat
3:   Iteration  $i$  begins
4:    $\mathbf{x}_0^i \leftarrow \mathbf{x}_0$ ,  $\mathcal{X}^i \leftarrow \mathbf{x}_0^i$ 
5:   while  $\|\mathbf{x}_t^i - \mathbf{x}_{\text{target}}\|_2 \geq \epsilon$  do
6:      $\mathbf{u}_t^i \leftarrow \text{Controller}(\mathbf{x}_t^i, \mathcal{C}_t^i, \mathcal{H})$ 
7:      $\mathbf{x}_{t+1}^i \leftarrow f(\mathbf{x}_t^i, \mathbf{u}_t^i)$ 
8:      $t \leftarrow t + 1$ 
9:      $\mathcal{X}^i \leftarrow \mathcal{X}^i \cup \mathbf{x}_t^i$ 
10:   end while
11:    $\mathcal{H} \leftarrow \mathcal{H} \cup \mathcal{X}^i$ 
12:    $i \leftarrow i + 1$ 
13: until Task is finished

```

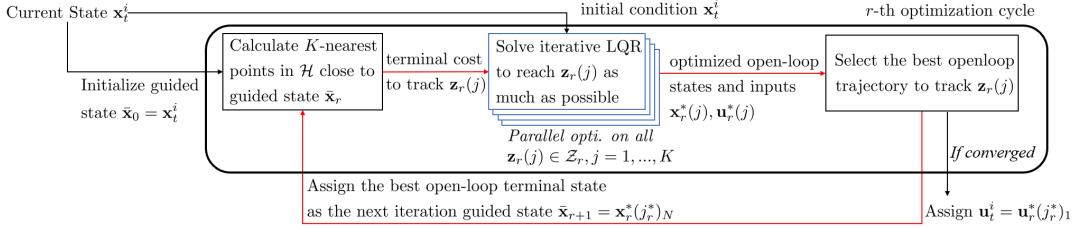
---

## III. ALGORITHM

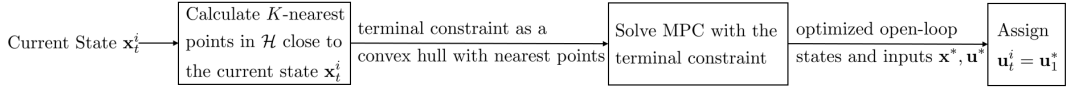
After introducing the problem setup for iterative tasks, the design of the proposed Iterative LQR for Iterative Tasks (i2LQR) in a dynamic environment will be presented in this section. The general idea of the algorithm will be introduced in Sec. III-A. Sec. III-B shows how to build a target terminal set using historical data. Details about the local iLQR optimization and best open-loop solution selection will be shown in Sec. III-C and Sec. III-D, respectively.

### A. Structure of i2LQR

Consider the problem of achieving the system's optimal performance for iterative tasks in a dynamic environment in the form of Alg. 1. The proposed control strategy i2LQR computes the optimal input using historical data from previous iterations. This includes states that the system has visited in previous iterations and the cost-to-go  $h(\mathbf{x}_t^i)$  associated with each historical state. In the first iteration, any open-loop controller could be used to generate a feasible trajectory. Then, the proposed i2LQR algorithm is deployed to calculate the system's optimal input at each time step. Fig. 1a shows the structure of the proposed algorithm. As a comparison, the structure of the LMPC algorithm is also presented in Fig. 1b.



(a) Proposed i2LQR. The optimization problem is resolved iteratively in the outer loop colored in red connected lines, and multiple iLQR problems are solved in parallel at each outer loop iteration colored in blue.



(b) LMPC [12], [13]. The key difference between LMPC and our proposed i2LQR is that performance optimal points are regarded as terminal constraints instead of terminal costs updated iteratively.

Fig. 1: Illustration of i2LQR and existing LMPC algorithms

Different from LMPC algorithm, the proposed i2LQR controller consists of several optimization cycles. For the  $r$ -th optimization cycle, we define a guided state  $\bar{x}_r$ , which will guide the position of the open-loop terminal state of the iLQR optimization (see Fig. 2). For the first cycle, the state at the current time step  $x_t^i$  will be used as the guided state, while the best open-loop predicted terminal state  $\mathbf{x}_{r-1}^*(j_{r-1}^*)_N$  from the last cycle will be used as the guided state for  $r$ -th cycle. Then  $K$ -nearest points to  $\bar{x}_r$  from the historical states set  $\mathcal{H}$  will build the target terminal set  $\mathcal{Z}_r$ , which consists the target terminal state  $\mathbf{z}_r(j)$  of the  $j$ -th iLQR optimization. To reduce the computational time of the proposed algorithm, these iLQR optimizations will be solved through parallel computing, colored in blue in Fig. 1a. Then the best open-loop predicted solution for the  $r$ -th optimization cycle will be selected. The algorithm will continue doing optimization until either the set  $\mathcal{Z}_r$  remains unchanged or the maximum cycle number  $r_{\max}$  is reached. As a result, the algorithm will select the iLQR's optimal target terminal state  $\mathbf{z}_r(j_r^*)$  from historical data in an iterative manner. Details about this algorithm will be illustrated in the following subsections.

### B. Nearest Points Selection

To build the target terminal set  $\mathcal{Z}_r$ , The following criteria will be used to select the  $K$ -nearest points:

$$J_{\mathbf{z}}(\bar{x}_r) = \min_{\mathbf{z}_r(j)} \sum_{j=1}^K \|\mathbf{z}_r(j) - \bar{x}_r\|_{D_0}^2 \quad (1a)$$

$$\text{s.t. } z_j \neq z_l, \forall j \neq l \quad (1b)$$

$$z_j \in \mathcal{H}, j = 1, \dots, K \quad (1c)$$

where  $j$  refers to the index of points in  $r$ -th optimization cycle;  $D_0$  is a diagonal matrix that contains weighting factors for state variables.

*Remark 1:* The number of maximum iteration  $r_{\max}$  and the number of selected nearest points  $K$  are the hyper-parameters of the proposed algorithm. A larger value of  $r_{\max}$  or  $K$  will make the system converge to the optimal

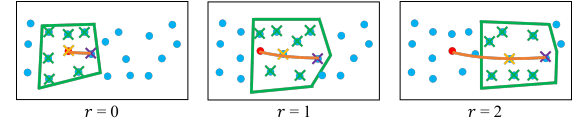


Fig. 2: An illustration of nearest points selection in an iterative manner. System state at the current time step is marked in red, while historical states are marked in blue. States on the right come with a smaller cost-to-go. Points with crosses are the selected nearest points in the corresponding optimization cycle. Specifically, yellow represents the guided state, and purple indicates the historical state for the best open-loop trajectory. The orange line is the best open-loop trajectory for the corresponding optimization cycle. In this way, the proposed i2LQR algorithm computes the optimal open-loop trajectory in an iterative manner.

performance more quickly. However, this will also increase the computational burden at each time step.

### C. Local iLQR Optimization

Following constrained finite-time optimal control problem will be solved through iLQR for each  $\mathbf{z}_r(j)$ :

$$J_l(\mathbf{x}_t^i, \mathbf{z}_r(j)) = \min_{\mathbf{u}_r^*(j)} p(\mathbf{x}_r^*(j)_{1+N}, \mathbf{z}_r(j)) \quad (2a)$$

$$\text{s.t. } \mathbf{x}_r^*(j)_{k+1} = f(\mathbf{x}_r^*(j)_k, \mathbf{u}_r^*(j)_k), k = 1, \dots, N \quad (2b)$$

$$\mathbf{x}_r^*(j)_{k+1}, \mathbf{u}_r^*(j)_k \in \mathcal{C}_{t+k|t}^i, k = 1, \dots, N \quad (2c)$$

$$\mathbf{x}_r^*(j)_1 = \mathbf{x}_t^i, \quad (2d)$$

where (2a) is the objective function of the optimization problem; (2b) represents the system dynamics; (2c) shows the constraints of the system along the prediction horizon; (2d) indicates the initial constraint. Specifically, the terminal cost introduces the difference between the open-loop predicted terminal state and the target terminal state in the quadratic form:

$$p(\mathbf{x}_r^*(j)_{1+N}, \mathbf{z}_r(j)) = (\mathbf{x}_r^*(j)_{1+N} - \mathbf{z}_r(j))^T P (\mathbf{x}_r^*(j)_{1+N} - \mathbf{z}_r(j)), \quad (3)$$

where  $P$  is a diagonal matrix consisting of weighting factors.

Alg. 2 shows how to solve the above optimization problem through iLQR. Constraints on states and inputs along the

prediction horizon will be converted to part of the new cost function  $J_s(\cdot)$  through the exponential function as done in [18]. As shown in Alg. 2, the algorithm starts with an initial input sequence, such as zero control inputs in this work. Then,  $g(\cdot)$  will calculate the open-loop states based on open-loop inputs and initial state through system dynamics (2b) during the forward pass at line 4. It will be linearized along with the cost function  $J_s(\cdot)$  around  $\mathbf{x}_r^m(j)$  and  $\mathbf{u}_r^m(j)$ . The optimal solution  $\delta^*(\mathbf{u}_r^m(j))$  could be obtained efficiently and will be used to generate the input sequence for the next iteration  $\mathbf{u}_r^{m+1}(j)$ . The algorithm will do this computation repeatedly until the cost  $J_s(\cdot)$  has converged or the maximum iteration  $m_{\max}$  is reached.

---

**Algorithm 2** iLQR

---

```

1:  $\mathbf{u}_r^0(j) \leftarrow \mathbf{0}$ 
2: repeat
3:   Iteration  $m$  begins
4:    $\mathbf{x}_r^m(j) \leftarrow g(\mathbf{x}_t^i, \mathbf{u}_r^m(j))$ 
5:   Linearize  $f(\cdot)$  and  $J_s(\cdot)$  around  $\mathbf{x}_r^m(j)$  and  $\mathbf{u}_r^m(j)$ 
6:    $\delta^*(\mathbf{u}_r^m(j)) \leftarrow \text{LQR}(\delta(\mathbf{x}_r^m(j)), \delta(\mathbf{u}_r^m(j)))$ 
7:    $\mathbf{u}_r^{m+1}(j) \leftarrow \mathbf{u}_r^m(j) + \delta^*(\mathbf{u}_r^m(j))$ 
8:    $m \leftarrow m + 1$ 
9: until Reach  $m_{\max}$  OR  $J_s(\cdot)$  has converged

```

---

#### D. Best Open-Loop Solution Selection

In each optimization cycle, the best open-loop solution will be selected among  $K$  solutions. Following local cost will be used in this process:

$$j_r^* = \underset{j=1, \dots, K}{\operatorname{argmin}} w_h h(\mathbf{z}_r(j_r)) + w_d \|\mathbf{x}_r^*(j_r) - \mathbf{z}_r(j_r)\|_{D_1}^2, \quad (4)$$

where  $w_h$ ,  $w_d$  are weighting factors;  $h(\cdot)$  is the cost-to-go associated with the state  $\mathbf{z}_r(j_r)$ ;  $\|\mathbf{x}_r^*(j_r) - \mathbf{z}_r(j_r)\|_{D_1}^2$  describes the penalty for the state difference between  $\mathbf{x}_r^*(j_r)$  and  $\mathbf{z}_r(j_r)$  with a diagonal weighting matrix  $D_1$ . Since cost-to-go function  $h(\cdot)$  is considered in (4), this allows the iterative optimization to find best terminal state in the outer loop of i2LQR, shown in red connected lines in Fig. 1a.

## IV. RESULTS

Having illustrated our optimal control strategy for iterative tasks in a dynamic environment in the previous sections, we now show the performance of the proposed algorithm. In Sec. IV-A, the basic setup for the simulation is introduced. Then, the performance of the proposed controller will be compared with state-of-the-art learning-based MPC algorithm: in the Sec. IV-B, results on iterative tasks in a static environment will be illustrated; in the Sec. IV-C, results on iterative tasks in a dynamic environment will be presented.

#### A. Simulation Setup

Nonlinear kinematic bicycle model with input constraints as in [18] will be used to evaluate the proposed algorithm.

$$\mathbf{x}_t = [x_t, y_t, v_t, \theta_t]^T, \quad \mathbf{u}_t = [a_t, \delta_t]^T, \quad (5)$$

are states and inputs vectors at time step  $t$ , respectively; specifically,  $x_t$  and  $y_t$  describe the system's position;  $v_t$  shows the system's speed;  $\theta_t$  indicates the heading angle;  $a_t$  introduces the acceleration;  $\delta_t$  represents the steering angle. In this work, the sampling time  $dt$  is set to 1 sec, which is consistent with the open-source code of [13]. The system is subject to the following input constraints:

$$-2 \text{ m/s}^2 \leq a_t \leq 2 \text{ m/s}^2, \quad -\frac{\pi}{2} \text{ rad.} \leq \delta_t \leq \frac{\pi}{2} \text{ rad.} \quad (6)$$

For each iteration, the initial state  $\mathbf{x}_0$  and target state  $\mathbf{x}_{\text{target}}$  are set to  $[0 \text{ m}, 0 \text{ m}, 0 \text{ m/s}, 0 \text{ rad.}]^T$  and  $[201.5 \text{ m}, 0 \text{ m}, 0 \text{ m/s}, 0 \text{ rad.}]^T$ , respectively. The cost-to-go  $h(\mathbf{x}_t^i)$  is the time to finish the corresponding iteration from the point  $\mathbf{x}_t^i$  to  $\mathbf{x}_{\text{target}}$ , which means that the algorithm aims to minimize the time to finish each iteration. In iteration 0, a brute force algorithm is used to calculate the initial feasible trajectory. This trajectory will be used by both i2LQR and LMPC algorithms for all simulations. In iteration 1, both algorithms will use the historical data from iteration 0, and historical data from the two previous iterations will be used by both algorithms in subsequent iterations. In this work, numerical simulation is implemented in Python. For the LMPC algorithm, CasADi [19] is used as modeling language and the resulting optimization is solved with IPOPT [20].

#### B. Iterative Tasks In Static Environments

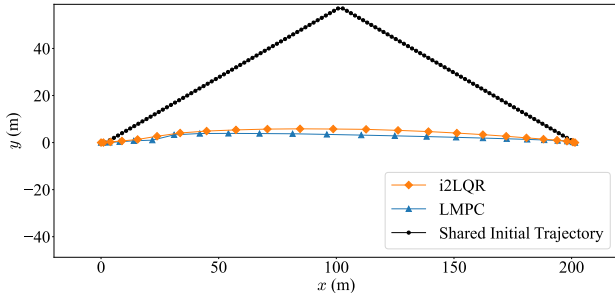
In order to compare the performance between our proposed i2LQR and LMPC for iterative tasks in a static environment, we do two groups of simulations.

In the first group of simulations, no obstacle exists in the environment. In each iteration, the system will travel from the initial state  $\mathbf{x}_0$  to the target state  $\mathbf{x}_{\text{target}}$ . The initial trajectory and trajectory in iteration 10 for the two algorithms are shown in Fig. 3a. Fig. 3b shows the timestamps to finish every single iteration using two algorithms. In Fig. 3c and Fig. 3d, the system's velocity and acceleration in iteration 10 using the two algorithms are presented.

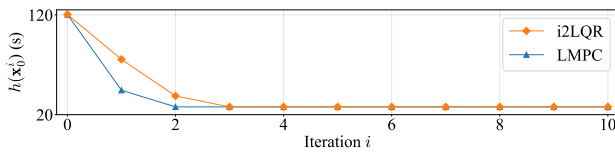
According to Fig. 3b, both i2LQR and LMPC algorithms minimize the time consumption for the system to reach the target state. The optimal time cost is the same for both algorithms. Specifically, given the same initial trajectory, the trajectories in iteration 10 will be straight lines between the initial state and target state for both algorithms. As shown in Fig. 3d, for both algorithms in iteration 10, the system will accelerate for the first half of the simulation and then decelerate to reach the target state with zero velocity.

In the second group of simulations, an ellipse-shaped static obstacle with center  $(x_{\text{obs}}, y_{\text{obs}}) = (100 \text{ m}, -5 \text{ m})$  exists in the environment. The system must travel from the initial state  $\mathbf{x}_0$  to the target state  $\mathbf{x}_{\text{target}}$  while avoiding the obstacle. Again, Fig. 4 shows the information for numerical simulations using the two algorithms.

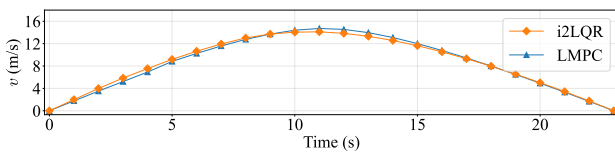
Fig. 4b shows that both i2LQR and LMPC algorithms minimize the time consumption for the system to reach the target state even a static obstacle exists in the environment. According to Fig. 4a, given the same initial trajectory, both algorithms can find the optimal trajectory that avoids the



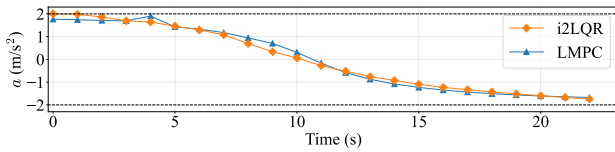
(a) Shared initial trajectory, and trajectories in iteration 10 for i2LQR and LMPC.



(b) Time to finish the iteration for i2LQR and LMPC.



(c) System speed in iteration 10 for i2LQR and LMPC.



(d) System acceleration in iteration 10 for i2LQR and LMPC.

Fig. 3: Simulation with no obstacle. Both algorithms could reach the system's optimal performance.

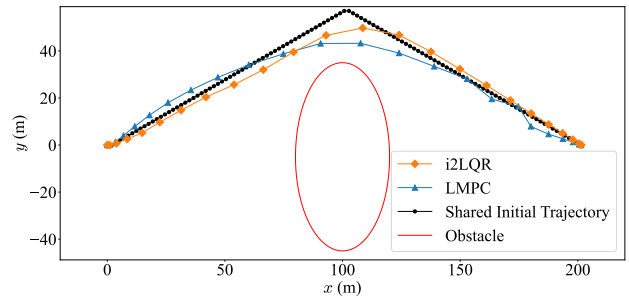
obstacle. According to Fig. 4d, in iteration 10, the system will accelerate for the first half of the simulation and then decelerate to reach the target state with zero velocity.

However, Fig. 4b shows that the times to finish the iteration are not stable for the i2LQR algorithm after the system reaches its optimal performance. This is due to the fact that all constraints are written in the form of the cost function. Numerical fluctuation may occur during this process.

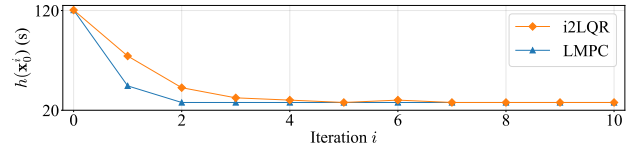
### C. Iterative Tasks In Dynamic Environments

To show the proposed i2LQR algorithm's performance for iterative tasks in dynamic environments, we conduct two groups of simulations with different environments.

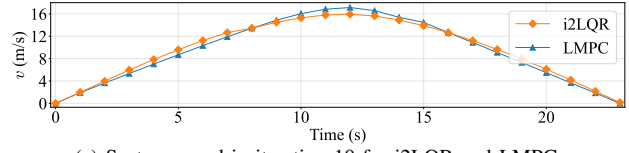
In the third group of simulations (Fig. 5), a static circle-shaped obstacle with center  $(x_{\text{obs}}, y_{\text{obs}}) = (35 \text{ m}, 0 \text{ m})$  exists in the environment for the iteration 6. According to Fig. 5b, systems with the both algorithms have reached their optimal performance before the static obstacle is introduced. During iteration 6, i2LQR spends 25 s to reach the target state while avoiding the static obstacle. Then, it returns to its optimal performance after the obstacle is removed. However, the LMPC cannot reach the target state after more than 100 s. The reason is that all the nearby historical states except the initial state are occupied by the obstacle, which results in the infeasibility of the optimization problem.



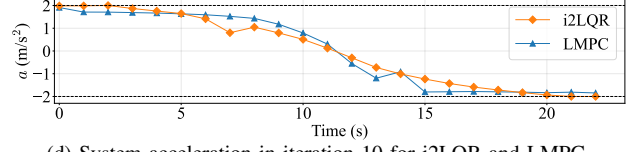
(a) Shared initial trajectory, and trajectories in iteration 10 for i2LQR and LMPC.



(b) Time to finish the iteration for i2LQR and LMPC.

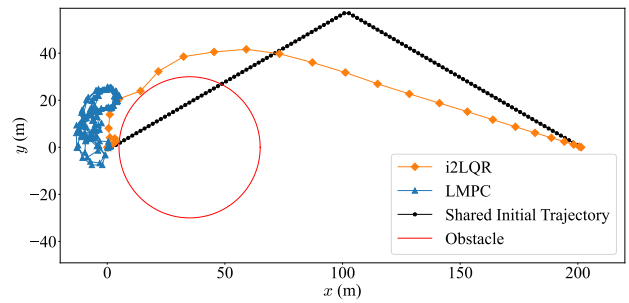


(c) System speed in iteration 10 for i2LQR and LMPC.

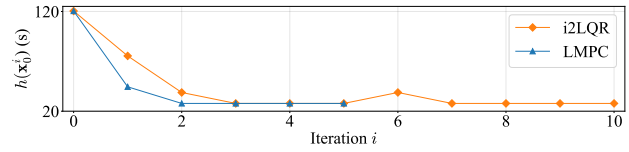


(d) System acceleration in iteration 10 for i2LQR and LMPC.

Fig. 4: Simulation with a static obstacle. Both algorithms could reach the system's optimal performance.

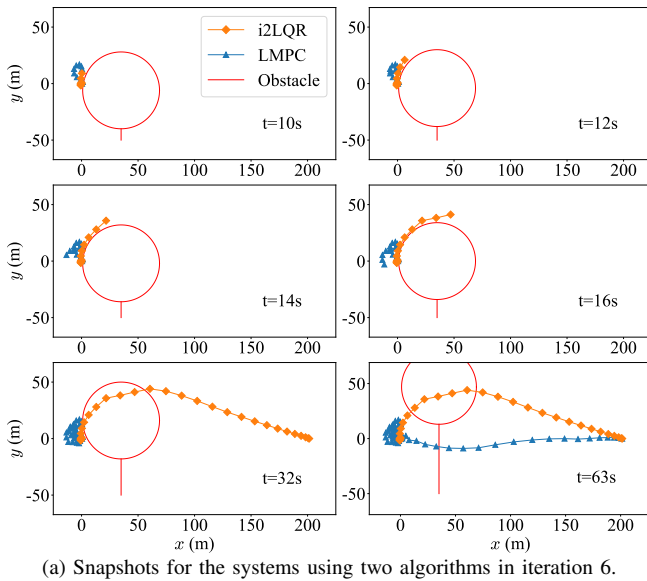


(a) Shared initial trajectory, and trajectories in iteration 6 for i2LQR and LMPC. The static obstacle is plotted in red.

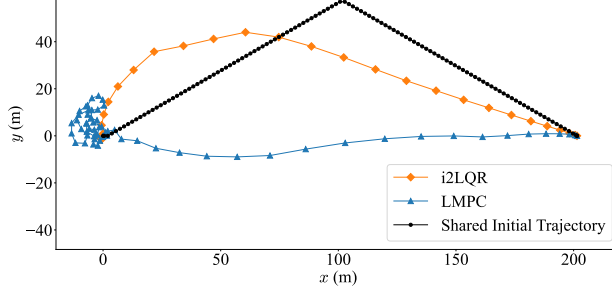


(b) Time to finish the iteration for i2LQR and LMPC.

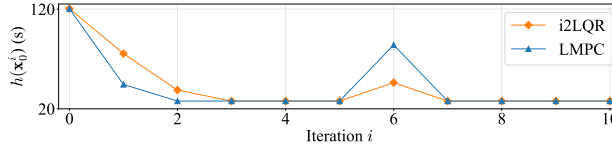
Fig. 5: Simulation with an added static obstacle in iteration 6. In iteration 6, the proposed i2LQR reaches the target state  $\mathbf{x}_{\text{target}}$  while the LMPC cannot reach the target state  $\mathbf{x}_{\text{target}}$ .



(a) Snapshots for the systems using two algorithms in iteration 6.



(b) Shared initial trajectory, and trajectories in iteration 6 for i2LQR and LMPC.



(c) Time to finish the iteration for i2LQR and LMPC.

Fig. 6: Simulation with an added moving obstacle in iteration 6. In iteration 6, the proposed i2LQR reaches the target state  $\mathbf{x}_{\text{target}}$  earlier than the LMPC, which means the system comes with a smaller cost-to-go  $h(\mathbf{x}_0^6)$ .

To further present the proposed i2LQR algorithm's performance in a more complicated dynamic environment, in the fourth simulation, a circle-shaped moving obstacle moves upwards from the initial point  $(x_{\text{obs}}, y_{\text{obs}}) = (35 \text{ m}, -16 \text{ m})$  with a speed of 1 m/s in iteration 6. The obstacle is removed in the next iteration. Fig. 6a and Fig. 6b show the snapshots and trajectories for both i2LQR and LMPC algorithms in iteration 6, respectively. It's shown that i2LQR is able to avoid this moving obstacle even when the obstacle is close to the system. However, since historical states with smaller time costs are occupied by the obstacle, these states become infeasible for the local MPC optimization of the LMPC algorithm; therefore, the controller cannot drive the system towards the target state at the beginning. After the obstacle goes away from the system, it moves towards the target state. According to Fig. 5b, both algorithms have reached their optimal performance before the moving obstacle exists.

The i2LQR spends 32 s to finish the iteration 6, while the LMPC spends 63 s to finish this in the same environment. Both algorithms return to their optimal performance after the moving obstacle is removed from the environment.

*Remark 2:* For the iterative task in a dynamic environment, it's possible to get a feasible solution by adding slack variables to the terminal state constraint of LMPC in [13]. This converts the hard constraints on the terminal state into cost-based soft constraints. However, using slack variables is not in line with the design of the LMPC algorithm, which relies on the feasibility of the target terminal state. Further more, the performance of the algorithm may not be guaranteed when slack variables are used.

## V. CONCLUSION

In this work, a control strategy called Iterative Linear Quadratic Regulator for Iterative Tasks (i2LQR) is presented. The proposed algorithm achieves the system's optimal performance for iterative tasks in dynamic environments. The algorithm utilizes historical data in an optimization problem, which will be solved in an iterative manner. To illustrate our control design, four sets of simulations are conducted. In the first two groups of simulations with a static environment, our proposed i2LQR algorithm provides the same optimal performance as state-of-the-art LMPC algorithm. In the remaining two simulations where the environment changes during the simulation, the i2LQR algorithm outperforms the LMPC algorithm. In future work, stability and feasibility analysis of the proposed controller will be presented.

## REFERENCES

- [1] A. Jain and M. Morari, "Computing the racing line using bayesian optimization," in 2020 59th IEEE Conference on Decision and Control (CDC). IEEE, 2020, pp. 6192–6197.
- [2] X. Wu, J. Zeng, A. Tagliabue, and M. W. Mueller, "Model-free online motion adaptation for energy-efficient flight of multicopters," *IEEE Access*, vol. 10, pp. 65 507–65 519, 2022.
- [3] N. R. Kapania, J. Subotsis, and J. Christian Gerdes, "A sequential two-step algorithm for fast generation of vehicle racing trajectories," *Journal of Dynamic Systems, Measurement, and Control*, vol. 138, no. 9, 2016.
- [4] A. Nagy and I. Vajk, "Sequential time-optimal path-tracking algorithm for robots," *IEEE Transactions on Robotics*, vol. 35, no. 5, pp. 1253–1259, 2019.
- [5] A. Heilmeier, A. Wischnewski, L. Hermansdorfer, J. Betz, M. Lienkamp, and B. Lohmann, "Minimum curvature trajectory planning and control for an autonomous race car," *Vehicle System Dynamics*, 2019.
- [6] A. Palleschi, M. Hamad, S. Abdolshah, M. Garabini, S. Haddadin, and L. Pallottino, "Fast and safe trajectory planning: Solving the cobot performance/safety trade-off in human-robot shared environments," *IEEE Robotics and Automation Letters*, vol. 6, no. 3, pp. 5445–5452, 2021.
- [7] F. Gao, L. Wang, B. Zhou, X. Zhou, J. Pan, and S. Shen, "Teach-repeat-replan: A complete and robust system for aggressive flight in complex environments," *IEEE Transactions on Robotics*, vol. 36, no. 5, pp. 1526–1545, 2020.
- [8] F. Fuchs, Y. Song, E. Kaufmann, D. Scaramuzza, and P. Dürr, "Superhuman performance in gran turismo sport using deep reinforcement learning," *IEEE Robotics and Automation Letters*, vol. 6, no. 3, pp. 4257–4264, 2021.
- [9] Y. Song, M. Steinweg, E. Kaufmann, and D. Scaramuzza, "Autonomous drone racing with deep reinforcement learning," in 2021 IEEE/RSJ International Conference on Intelligent Robots and Systems (IROS). IEEE, 2021, pp. 1205–1212.

- [10] R. Penicka, Y. Song, E. Kaufmann, and D. Scaramuzza, “Learning minimum-time flight in cluttered environments,” *arXiv preprint arXiv:2203.15052*, 2022.
- [11] J. Kabzan, L. Hewing, A. Liniger, and M. N. Zeilinger, “Learning-based model predictive control for autonomous racing,” *IEEE Robotics and Automation Letters*, vol. 4, no. 4, pp. 3363–3370, 2019.
- [12] U. Rosolia and F. Borrelli, “Learning model predictive control for iterative tasks. a data-driven control framework,” *IEEE Transactions on Automatic Control*, vol. 63, no. 7, pp. 1883–1896, 2017.
- [13] ——, “Minimum time learning model predictive control,” *International Journal of Robust and Nonlinear Control*, vol. 31, no. 18, pp. 8830–8854, 2021.
- [14] ——, “Learning how to autonomously race a car: a predictive control approach,” *IEEE Transactions on Control Systems Technology*, vol. 28, no. 6, pp. 2713–2719, 2019.
- [15] Y. Kim, S. Tay, J. Guanetti, and F. Borrelli, “Eco-driving with learning model predictive control,” *arXiv preprint arXiv:1907.04990*, 2019.
- [16] G. Li, A. Tunchez, and G. Loianno, “Learning model predictive control for quadrotors,” in *IEEE International Conference on Robotics and Automation*, 2022.
- [17] S. He, J. Zeng, and K. Sreenath, “Autonomous racing with multiple vehicles using a parallelized optimization with safety guarantee using control barrier functions,” in *IEEE International Conference on Robotics and Automation*, 2022.
- [18] J. Chen, W. Zhan, and M. Tomizuka, “Constrained iterative lqr for on-road autonomous driving motion planning,” in *2017 IEEE 20th International Conference on Intelligent Transportation Systems (ITSC)*. IEEE, 2017, pp. 1–7.
- [19] J. A. Andersson, J. Gillis, G. Horn, J. B. Rawlings, and M. Diehl, “Casadi: a software framework for nonlinear optimization and optimal control,” *Mathematical Programming Computation*, vol. 11, no. 1, pp. 1–36, 2019.
- [20] L. T. Biegler and V. M. Zavala, “Large-scale nonlinear programming using ipopt: An integrating framework for enterprise-wide dynamic optimization,” *Computers & Chemical Engineering*, vol. 33, no. 3, pp. 575–582, 2009.